



Artificial neural network prediction of exhaust emissions and flame temperature in LPG (liquefied petroleum gas) fueled low swirl burner



Bamiji Z. Adewole^{a,*}, Olatunde A. Abidakun^b, Abraham A. Asere^a

^a Thermo-fluids and Energy Research Group, Department of Mechanical Engineering, Obafemi Awolowo University, Ile-Ife, Nigeria

^b Department of Mechanical Engineering, Covenant University, Ota, Ogun State, Nigeria

ARTICLE INFO

Article history:

Received 16 May 2013

Received in revised form

12 August 2013

Accepted 16 August 2013

Available online 24 September 2013

Keywords:

ANN

Swirl burner

Liquefied petroleum gas

Emissions

Flame temperature

ABSTRACT

This study deals with ANN (artificial neural network) modeling of a swirl burner. The model was used to predict the flame temperature and pollutant emissions (CO (carbon monoxide) and NO_x (nitrogen oxide)) from combustion of LPG (liquefied petroleum gas) in the swirl burner. The data for the training and testing of the proposed ANN was obtained by combusting LPG at various equivalent ratios (LPG/air ratios) and swirler's vane angles in a low swirl burner. Vane angles of 35–60° in steps of 5° and equivalent ratios of 0.94, 0.90, 0.85, 0.80, 0.75, 0.71, 0.66 and 0.61 were considered. An ANN model based on standard back-propagation algorithms for the swirl burner was developed using some of the experimental data for training and validation. The performance of the ANN was tested by comparing the predicted outputs with the experimental values that were not used in training the network. *R* values of 0.94 were obtained for CO and NO_x and 0.99 for flame temperature. These results show that very strong correlation exists between the ANN predicted values and the experimental results. Therefore, this study demonstrates that the performance and emissions of swirl burner can be accurately predicted using ANN approach.

© 2013 Elsevier Ltd. All rights reserved.

1. Introduction

Preference for LPG (liquefied petroleum gas) in domestic and industrial heating appliances is predicated on its comparatively clean combustion product as it does not produce visible emissions [1]. However, it produces gaseous pollutants such as NO_x (nitrogen oxides) and CO (carbon monoxide) when its combustion devices are not efficient. The negative impact of these pollutants on the environment is of global concern [2], hence, various combustion and post combustion techniques [3] are being employed by combustion engineers to reduce these harmful emissions to acceptable levels [4].

Efficient combustion of LPG requires the use of appropriate equipment to produce turbulent mixing of atomized fuel and oxidant for achieving high efficiency in combustors [5]. This proper mixing of the constituents provided by high aerodynamic flow gives good combustion and produces lower pollutant emission. It also generates high temperature for total release of the fuels net calorific value [6]. Inefficient combustion leading to high emission of pollutants in the flue gas results where this turbulence and proper mixing could not be achieved due to design shortcomings.

Hence, the injection of fuel and oxidant through swirler is used to impart turbulence on the charge with a view to achieving high combustion efficiency [7,8].

Knowing the performance of a burner for different range of operating conditions is usually desired by manufacturers and combustion engineers. This requirement is either met by conducting a comprehensive experimental study or by modeling the burner operation [9]. Testing the burner under all possible operating conditions and fuel cases is practically impossible as it is both time consuming and expensive. Also, developing an accurate model for the operation and combustion dynamics in a burner system is difficult due to the complex processes involved [10]. As an alternative, the performance and exhaust emissions of a swirl burner can be modeled using ANN (artificial neural network). This modeling technique can be applied to estimate desired output parameters when enough experimental data is provided.

ANN can be used to model physical phenomena with simple mathematical representations. Prediction of ANN is achieved from training on experimental data which can be validated by independent data sets [11]. Selection of an appropriate neural network topology is therefore very important in terms of model accuracy and model simplicity.

Various researchers have shown ANN as a powerful modeling tool for predicting complex relationships. The ANNs approach has

* Corresponding author. Tel.: +234 8035026452.

E-mail address: akinbam2@yahoo.com (B.Z. Adewole).

been applied to predict the performance of various thermal and energy systems. Investigation of the performance of solar air collectors [12] and prediction of the bottom ash formed in a coal-fired power plant [13] were done using artificial neural network. ANN modeling was also applied in assessing [14] and in estimating the performance [15] of ground coupled heat pump systems used for cooling and heating purposes. Ref. [16] employed artificial neural networks for analyzing energy and predicting greenhouse basil production. ANN has also been found efficient in estimating the maximum power [17] and the annual energy produced [18] by a photovoltaic generator.

The performance and exhaust emissions in spark ignition engine using ethanol-gasoline blends were done by Ghobadian [19] using ANN prediction. It was concluded that ANN provided the best accuracy in modeling the performance and emission indices. Ref. [20] utilized ANNs to predict specific fuel consumption and exhaust temperature for a diesel engine. Likewise Ref. [21], used ANN to predict the performance and exhaust emissions of a gasoline engine. Ref. [22] also analyzed the effect of octane number on exhaust emissions from engine using artificial neural network. They all concluded engine performance, exhaust emissions and exhaust gas temperature can be predicted by ANN model quite well.

In this study, the use of ANN has been proposed to determine CO emission, NO_x emission and flame temperature obtained from the combustion of LPG at different fuel equivalence ratio and swirler vane angles using results from experimental analysis.

2. Experimentation

2.1. Description of the experimental setup

The sectional view of the swirl burner experimental rig is shown in Fig. 1. The set-up consists of a swirl burner, air compressor, gas cylinder, fuel and air flow lines, rotameters, combustion exhaust chamber, temperature measuring devices, gas analyzer and digital camera. Omega rotameters calibrated in liter per minutes were used to independently measure the air and LPG flow rates into the swirl burner's pre-mix duct. The swirl burner was specifically designed to properly mix the gaseous fuel with the compressed air coming from a compressor (2.5 hp, 1500 W, 8 atm, 2800 rpm, POMA Air Compressor, ISO 9001:2000). The temperature distributions at the outlet of the swirl burner were measured using type K, mineral insulated grounded junction, 1.6 mm diameter thermocouple. The thermocouple which is capable of reading temperature of up to

1200 °C was connected to a digital read-out device. Gas sampling probe was inserted into the exhaust chamber and the composition of the exhaust gas was determined by using a gas analyzer (Eclipse EGA4 Combustion analyzer). The analyzer is capable of measuring oxides of nitrogen (NO_x) and carbon monoxides (CO).

2.2. Testing procedure

Tests on the swirl burner were carried out using six swirlers with different vane angles. Experiments were carried out using LPG which has composition of 75% butane and 25% propane as a fuel and air as a charge. Air and fuel were supplied into the pre-mixed duct of the swirl burner through the flow lines. Quantities of fuel and compressed air required to achieve desired equivalence ratios for combustion were measured using rotameters. Variations of the equivalence ratio were obtained by changing fuel flow rate while maintaining constant air flow rate. Each swirler was placed inside the swirl burner to impact a swirling flow onto the various air/fuel mixture for efficient combustion. Data on pollutant emissions and flame temperature were collected for vane angles from 35 to 60° in steps of 5° and equivalence ratios from 0.65 to 1.0 in steps of 0.5.

3. Experimental results

3.1. NO_x and CO emissions

Fig. 2 represents a variation of NO_x emissions from the combustion of LPG in the swirl burner with equivalence ratio at different vane angles. NO_x emissions lower than 5 ppm were obtained for the range of operating equivalence ratios (0.61 ≤ ϕ ≤ 0.95). The minimum NO_x emission of 0.33 ppm was obtained at swirler's vane angle of 55°. It represents a total NO_x reduction of 93.4% at equivalence ratio of 0.90.

Fig. 3 presents the profile of carbon monoxide emissions with equivalence ratio for all vane angles. CO emissions of less than 300 ppm were obtained for the range of operating equivalent ratios considered. Performance testing of vane swirlers revealed that CO emission level was drastically reduced to 45 ppm at equivalence ratio of 0.66 for swirler with vane angle of 55°. This value represents a reduction of 85% in total CO emission. However, at equivalence ratio of 0.90, CO emission was higher for swirler with vane angles of 35°, 45° and 50°, indicating inefficient combustion. This resulted from poor mixing of combustion reactants in comparison with vane angle of 55° and 60° at the same equivalence ratio. Reduction of 55.3% and 82.1% in carbon monoxide (CO) emissions

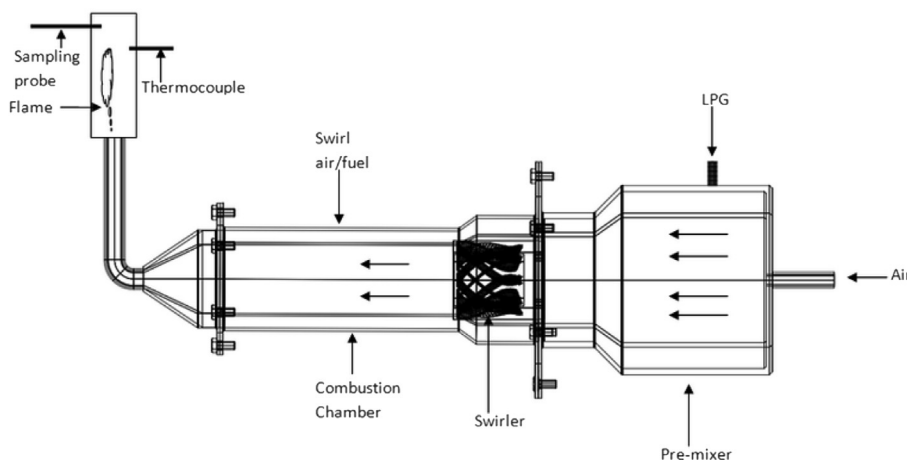


Fig. 1. Sectional view of the swirl burner experimental rig.

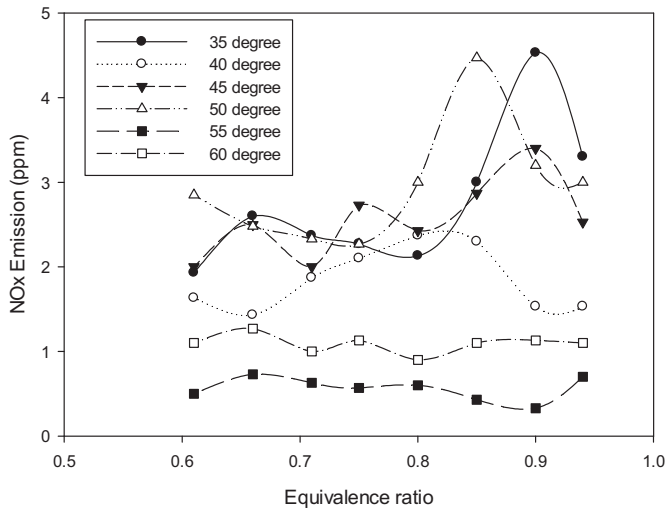


Fig. 2. Variation of NO_x emissions with equivalence ratio for various vane angles.

for swirler with vane angle of 60° and 55° respectively was observed at 0.90 equivalent ratio. From these results, it was observed that NO_x and CO emissions were strongly influenced by equivalence ratio and swirl intensity imparted by the swirler.

3.2. Flame temperature

Fig. 4 presents temperature profiles of the produced flame in the swirl burner. The trend here is similar to the trend exhibited in the plot of adiabatic flame temperature versus equivalence ratio for a methane–air mixture [23]. Increment in flame temperature with equivalence ratio towards fuel-rich side was noticed. Generally, for all swirlers, flame temperature reaches its peak value at an equivalence ratio where there is a good mixing and efficient combustion of fuel in the combustor. The maximum flame temperature (T_f) of 1096°C obtained was at swirler vane angle of 45° and equivalence ratio of 0.71. However, operating equivalence ratio of 0.90 and swirler's vane angle of 55° were selected as optimum. The selected optimum condition produced NO_x of 0.33 and CO of 53.7 ppm with flame temperature of 1012°C .

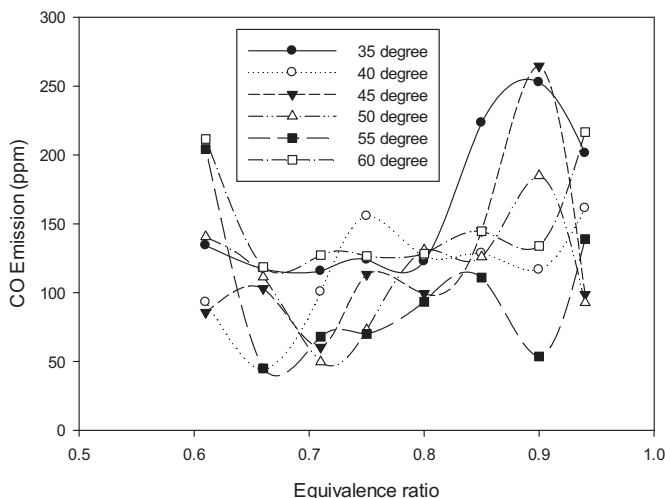


Fig. 3. Variation of CO emission with equivalence ratio for various vane angles.

4. Artificial neural networks

ANN's ability to acquire, store and utilize knowledge, likened to human information processing systems relies on its massively interconnected neurons. It can accurately predict outputs of a set of inputs by learning the pattern of experimental data and as such adjust itself [24]. Its application in modeling of systems where complex interaction exists among the input parameters is informed by this ability. The process of operation involves acceptance of sets of inputs by each of the neurons and subsequent output of the correlated response. Choice of appropriate learning method and training functions is needed in establishing perfect input to output relationship. The weight and biases attached to the set of inputs are continuously adjusted until the comparison of the ANN outputs meets certain criteria.

The performance of the ANN-based predictions is evaluated by regression analysis of the network outputs (predicted parameters) and the target outputs (experimental values). The correlation coefficient (R) is used to assess the strength of this relationship. The value of R ranges from -1 to $+1$ with values closer to $+1$ indicating a stronger positive linear relationship.

Errors between the network outputs (y) and the target outputs (t) are measured by some performance functions used for ANNs training. Among them are the RMSE (root mean squared error), MSE (mean squared error) and MRE (mean relative error). They are calculated as defined in equations (1)–(3) [11,21,25].

$$\text{MSE} = \frac{1}{N} \sum_{i=1}^N (y_i - t_i)^2 \quad (1)$$

$$\text{MRE}(\%) = \frac{1}{N} \sum_{i=1}^N \left| 100 \frac{(y_i - t_i)}{y_i} \right| \quad (2)$$

$$\text{RMSE} = \sqrt{\frac{1}{N} \sum_{i=1}^N (y_i - t_i)^2} \quad (3)$$

where N is the number of the data used for validation, t and y are actual output and predicted output sets, respectively.

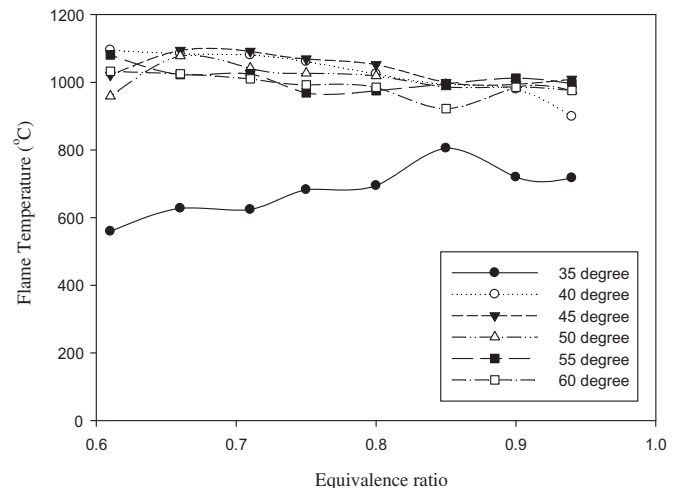


Fig. 4. Variation of flame temperature with equivalence ratio at different vane angles.

5. Modeling with ANN

An ANN model for the swirl burner was developed using data gathered from combustion of liquefied petroleum gas in a low swirl burner. The model was developed to predict the correlation between NO_x emission, CO emission and flame temperature using different vane angles and equivalent ratios (LPG-air ratio). In creating the model, 70% of the data set was randomly assigned as the training and validation set, while the remaining 30% was employed for testing the network performance.

Schematic representation of the ANN architecture for the swirl burner is shown in Fig. 5. There were two input and three output parameters in the experimental tests. The inputs to the ANN are the vane angles and equivalent ratios, whilst, the outputs are the CO emission, NO_x emission and the flame temperature. Hence, the input layer consisted of 2 neurons while the output layer had 3 neurons.

The number of hidden layers and the number of neurons in each of the hidden layers are part of the network features responsible for its performance. In view of this, various ANN configurations were trained, evaluated and tested (Table 1). Both feed forward and cascade forward (written as ff and cf in Table 1) networks were tested to permit selection of the most appropriate. The network topography in Table 1 refers to the number of neurons in the input layer, hidden layer(s) and output layer. Activation functions tan/lin or log/lin means the tansigmoid or logsigmoid transfer function was used in the hidden layer(s) while purelin was used in the output layer. All the ANN models were trained using standard back-propagation algorithm in which network weights and biases were initialized randomly at the beginning of the training phase. Mean squared error (MSE) which is the average squared error between the network outputs and the targets on the validation set was used as the stop criteria for model generalization.

A cascade-forward back propagation network was selected as the optimum network. Cascade forward is similar to feed-forward networks, but different in terms of the weight connections from the input to each layer and from each layer to the successive layers. As depicted in Table 1, the cascade forward networks consistently gave lower error condition compared to the feed forward networks. The selection decision was based on simplicity, low error condition and high coefficient of variation (R).

The network consists of two hidden layers with 12 neurons in the first and 13 neurons in the second. Hyperbolic tangent sigmoid (tansig) function was used as the transfer function in the hidden layers while the output layer was made up of pure linear (purelin) transfer function. The weight/bias coefficients adjustment and

Table 1

Summary of various networks evaluated to yield the criteria of network performance.

Network	Activation function	Training rule	Network topography	Testing error	R
ff	tan/lin	trainlm	(2,13,3)	491	0.99045
ff	log/lin	trainlm	(2,15,3)	229	0.9926
ff	tan/lin	trainlm	(2,15,3)	280	0.99433
ff	log/lin	trainbr	(2,20,3)	6×10^4	0.99625
ff	log/lin	trainlm	(2,20,3)	1.56×10^3	0.99106
ff	tan/lin	trainbr	(2,20,3)	1.19×10^4	0.99563
ff	tan/lin	trainlm	(2,20,3)	228	0.98572
ff	log/lin	trainlm	(2,8,8,3)	3.57×10^3	0.99322
ff	tan/lin	trainlm	(2,10,10,3)	341	0.99693
ff	tan/lin	trainlm	(2,11,11,3)	776	0.98928
cf	tan/lin	trainlm	(2,20,3)	0.000243	0.99372
cf	tan/lin	trainlm	(2,10,12,3)	8.31×10^{-26}	0.98604
cf	tan/lin	trainlm	(2,10,15,3)	3.76×10^{-11}	0.99226
cf	tan/lin	trainlm	(2,12,13,3)	4.99×10^{-11}	0.99287
cf	tan/lin	trainlm	(2,12,15,3)	3.41×10^{-11}	0.99662

error minimization process were achieved by using Levenberg-Marquardt (trainlm) training algorithm and gradient descent with momentum rule (learnngdm) respectively. The back-propagation and monitoring of the network performance were implemented under MATLAB 2010a environment.

6. Results and discussion

Based on the result of the ANN modeling, the training algorithm of back propagation was adequate for predicting CO emission, NO_x emission and flame temperature. The output parameters (predicted) from the ANN network of the swirl burner as a function of the experimental ones (target) are as shown in Figs. 6–8. In the graphs, the accuracy of the ANN predictions was evaluated by their closeness to the straight dashed line which indicates the perfect prediction. The high correlation between the ANN predicted values and the experimental values illustrated in the graphs implies that the model succeeded in predicting the performance and emissions.

The predicted versus target values for the CO and NO_x emissions are as shown in Figs. 6 and 7. The plots yield a correlation coefficient (R -values) of 0.94 for both CO and NO_x emissions. Fig. 8 shows the ANN-predicted versus experimental values for the flame temperature with correlation coefficient of 0.99. These values indicate existence of strong correlation in the modeling of swirl burner flame temperature and emissions. The created network has also shown the capability of predicting these parameters separately.

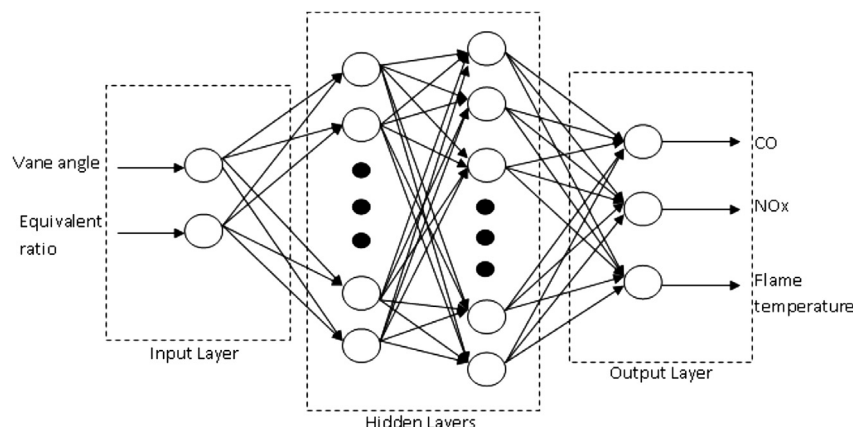


Fig. 5. Schematic representation of the ANN architecture for swirl burner.

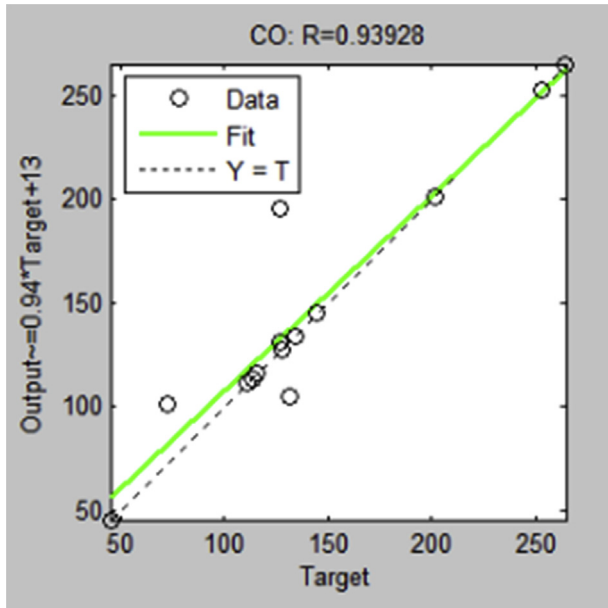


Fig. 6. ANN prediction versus the experimental values for CO.

Comparison of the output obtained by simulating the ANN and the target values for the set of 14 test data are shown in Figs. 9–11. The closeness of the curves further confirms the capability of ANN in predicting the CO emission, NO_x emission and flame temperature for swirl burner adequately.

7. Conclusion

An experimental study and artificial neural network modeling of LPG fueled swirl burner were performed to predict the flame temperature, NO_x and CO emissions of the burner. The swirling effect produced by swirlers of different vane angles at different equivalence ratios revealed that NO_x and CO emissions and flame temperature were strongly influenced by equivalence ratio and swirl intensity imparted by the swirler. The use of swirler with vane

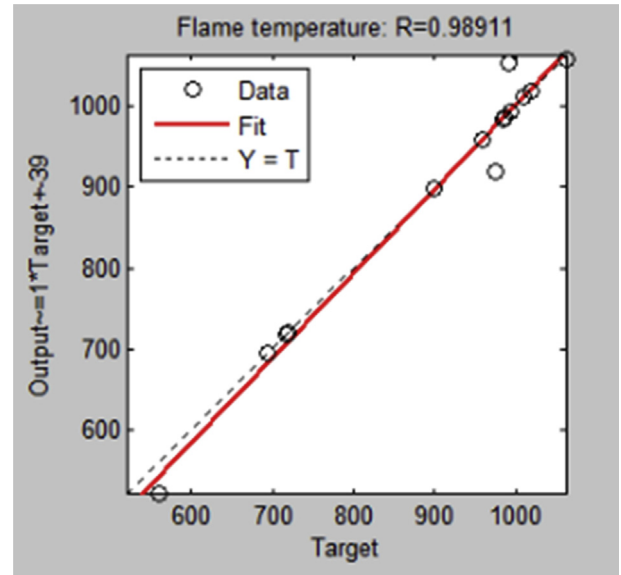


Fig. 8. ANN predictions versus experimental values for flame temperature.

angle of 55° at equivalence ratio of 0.90 allows the burner to operate at temperature of 1012 °C with minimum pollutant emissions of 0.33 for NO_x and 53.7 ppm for CO.

The performance of the cascade forward back propagation neural network was evaluated by the correlation coefficient and the

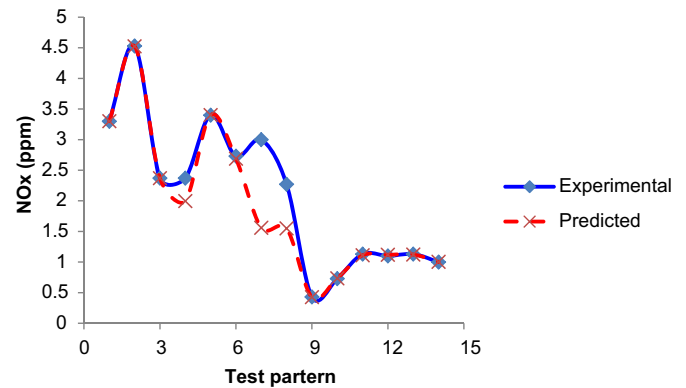


Fig. 9. Comparisons of experimental results and the ANN predictions for NO_x at various test patterns.

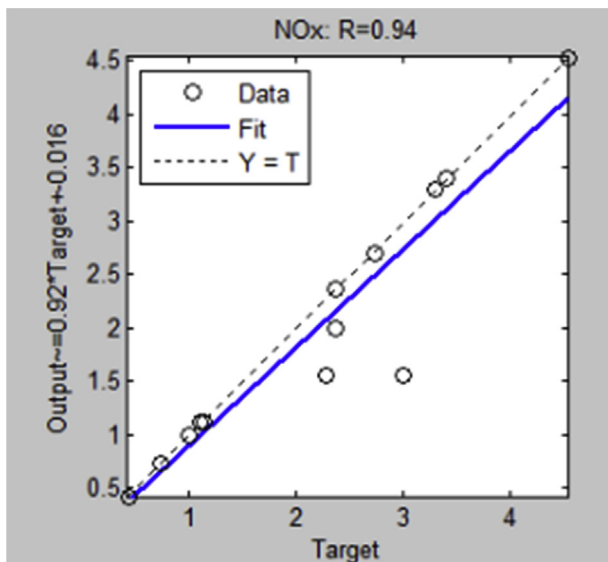


Fig. 7. ANN predictions versus the experimental values for NO_x.

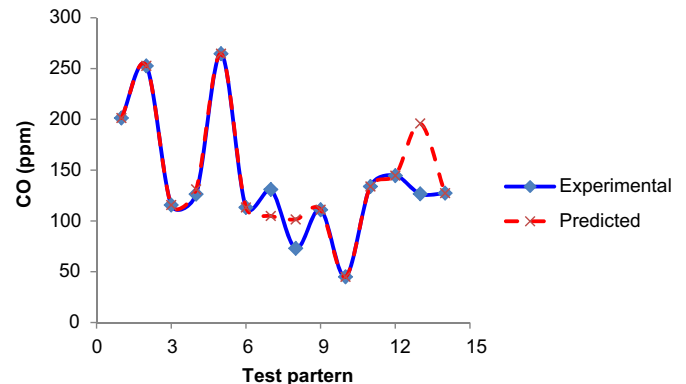


Fig. 10. Comparisons of experimental results and the ANN predictions for CO at various test patterns.

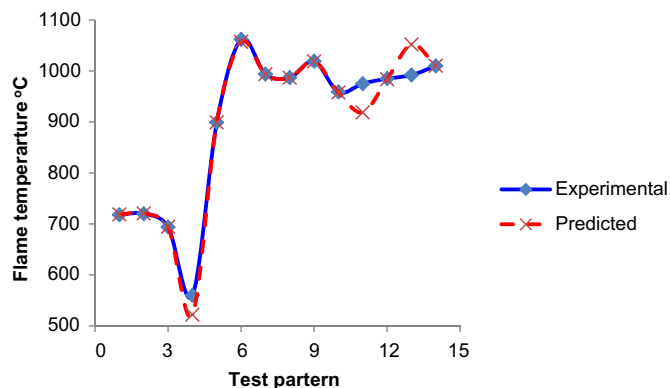


Fig. 11. Comparisons of experimental results and the ANN predictions for flame temperature at various test patterns.

mean square error (MSE). The very good, R values and very low MSE obtained showed that the neural network model was capable of learning the relationships among the input and output variables for the given data set. Plot and comparison of the ANN-predicted results and the experimental data showed good correlation. Hence, ANN proved to be a useful tool that can be employed in correlation and simulation of combustion parameters.

References

- [1] Tira HS, Herreros JM, Tsolakis A, Wyszynsk ML. Characteristics of LPG-diesel dual fuelled engine operated with rapeseed methyl ester and gas-to-liquid diesel fuels. *Energy* 2012;47(1):620–9.
- [2] Wang P, Wu W, Zhu B, Wei Y. Examining the impact factors of energy-related CO₂ emissions using the STIRPAT model in Guangdong Province, China. *Appl Energy* 2013;106:65–71.
- [3] Dupont V, Pourkashanian M, Williams A, Woolley R. The reduction of NO_x formation in natural gas burner flames. *Fuel* 1993;72(4):497–503.
- [4] Kumaran K, Shet USP. Effect of swirl on lean flame limits of pilot – stabilized open premixed turbulent flames. *Combust Flame* 2007;151:391–5.
- [5] Mujeebu MA, Abdullah MZ, Abu Bakar MZ, Mohamad AA, Abdullah MK. Applications of porous media combustion technology – a review. *Appl Energy* 2009;86(9):1365–75.
- [6] Huang Y, Yang V. Dynamics and stability of lean-premixed swirl-stabilized combustion. *Prog Energy Combust Sci* 2009;35(4):293–364.
- [7] Cheng RK, Yegian DT, Miyasato MM, Samuelsen GS, Benson CE, Pellizzari R, et al. Scaling and development of low-swirl burners for low-emission furnaces and boilers. *Proc Combust Inst* 2000;28(1):1305–13.
- [8] Xiouris CZ, Koutmos P. Fluid dynamics modeling of a stratified disk burner in swirl co-flow. *Appl Therm Eng* 2012;35:60–70.
- [9] Baukal CE. *Industrial burners handbook*. Boca Raton, Florida: CRC Press; 2003. p. 328–32.
- [10] Gokhale S, Khare M. A review of deterministic, stochastic and hybrid vehicular exhaust emission models. *Int J Transport Manag* 2004;2(2):59–74.
- [11] Kalogirou SA. Application of artificial neural-networks for energy systems. *Appl Energy* 2000;67:17–35.
- [12] Murat Caner M, Gedik E, Kecebas A. Investigation on thermal performance calculation of two type solar air collectors using artificial neural network. *Expert Syst Appl* 2011;38(3):1668–74.
- [13] Bekat T, Erdogan M, Inal F, Genc A. Prediction of the bottom ash formed in a coal-fired power plant using artificial neural networks. *Energy* 2012;45:882–7.
- [14] Esen H, Inalli M, Sengur A, Esen M. Artificial neural networks and adaptive neuro-fuzzy assessments for ground-coupled heat pump system. *Energy Build* 2008;40:1074–83.
- [15] Esen H, Inalli M. Modeling of a vertical ground coupled heat pump system by using artificial neural networks. *Expert Syst Appl* 2009;36:10229–38.
- [16] Pahlavan R, Omid M, Akram A. Energy input-output analysis and application of artificial neural networks for predicting greenhouse basil production. *Energy* 2012;37:171–6.
- [17] Almonacid F, Fernandez EF, Rodrigo P, Perez-Higueras PJ, Rus-Casas C. Estimating the maximum power of a high concentrator photovoltaic (HCPV) module using an artificial neural network. *Energy* 2013;53:165–72.
- [18] Almonacid F, Rus C, Perez-Higueras P, Hontoria L. Calculation of the energy provided by a PV generator. Comparative study: conventional methods vs. artificial neural networks. *Energy* 2011;36:375–84.
- [19] Ghobadian B, Kiani M, Tavakoli T, Nikbakht AM, Najafi G. Application of artificial neural networks for the prediction of performance and exhaust emissions in SI engine using ethanol-gasoline blends. *Energy* 2010;35:65–9.
- [20] Parlak A, Islamoglu Y, Yasar H, Egrisogut A. Application of artificial neural network to predict specific fuel consumption and exhaust temperature for a diesel engine. *Appl Therm Eng* 2006;26:824–8.
- [21] Canakci M, Sayin C, Ertunc HM, Hosoz M, Kilicasian I. Performance and exhaust emissions of a gasoline engine using artificial neural network. *Appl Therm Eng* 2007;27:46–54.
- [22] Yuanwang D, Meilin Z, Dong X, Xiaobei C. An analysis for effect of octane number on exhaust emissions from engine with the neural network. *Fuel* 2003;81:1963–70.
- [23] Duun-Rankin D. *Lean combustion technology and control*. Boulevard, UK: Elsevier Science Ltd; 2008.
- [24] Hagan MT, Demuth HB. *Neural network design*. Boston, USA: PWS Publishing Company; 1995.
- [25] Looney CG. *Pattern recognition using neural networks: theory and algorithms for engineers and scientists*. New York, USA: Oxford University Press; 1997.